

Statistical Approach for Modeling Connectors in SI-POF Avionics Systems

Alicia López¹, Angeles Losada¹, Dwight Richards², Javier Mateo¹, Xin Jiang², N. Antoniadis²

¹ *Photonic Technologies Group (GTF), Aragón Institute of Engineering Research (i3A),
Universidad de Zaragoza, Zaragoza, Spain*

² *Department of Engineering and Environmental Science, College of Staten Island,
The City University of New York, Staten Island, NY 10314 USA*

Tel: +34 876 555566, Fax: +34 976 762111, e-mail: aliclope@unizar.es

ABSTRACT

The application of Plastic Optical Fibers (POF) as transmission medium in avionics systems requires the introduction of a number of connections that affect both the power budget and the system bandwidth. Additionally, the use of air-gap connectors in order to avoid fiber damage by physical contact through the vibrations induces statistically variable positional shifts that add to the already large variability present in POF-based systems. Therefore, it is important to incorporate connector variability to obtain realistic simulation results of the performance of POF avionics links. Our aim here is to evaluate the impact of this variability on transmission properties by using a connector model that includes lateral and longitudinal offsets and performing Monte Carlo simulations of several avionics scenarios using a POF propagation matrix framework.

Keywords: Plastic optical fibers, avionics systems, statistical analysis, optical communications.

1. INTRODUCTION

The application of Plastic Optical Fibers (POFs) in short-haul environments such as networks inside a car, a home or an airplane, generally requires the introduction of a large number of connections [1]. POF connector losses have been experimentally measured for different types of connectors and fiber termination procedures and found to be rarely below 1 dB [2]. A connector model based on an experimental characteristic matrix was proposed and validated using experimental results [3]. This model was integrated into a propagation matrix framework demonstrating that, in a POF link, connectors do not only reduce the power budget but also change the system bandwidth, depending on their positions, in agreement with experimental results [4,5]. In addition, misalignments are difficult to avoid or may be intentionally introduced as a feature in connectors with no physical contact, further limiting the already compromised power budget. Vibrations, which are frequent in transportation environments, are also the source of statistically variable positional shifts. Therefore, a method to estimate lateral and longitudinal misalignment losses based on the calculation of the radiated angular power distribution using the Hankel transform was proposed to upgrade the connector matrix model [6]. Also, a methodology for engineering SI-POF and connectors, developed by integrating the matrix framework into commercial software, was applied to evaluate the performance of a typical avionics system that included a number of connectors [7]. A similar approach was applied to evaluate several designs for automotive Ethernet over POFs incorporating lateral misalignments [8]. If the maximum fiber misalignment based on typical tolerances of standard SI-POFs is used, a very conservative estimate of system performance would be obtained. Instead, a model that estimates the statistical properties of the system parameters should be used to obtain more realistic simulation results. Along this line, a statistical analysis of coupling loss due to diameter and numerical aperture mismatches as well as offsets in all possible axes was performed by Monte Carlo simulations [9,10]. Our aim is to pursue a similar approach, but extending the statistical analysis to other transmission parameters, such as system bandwidth, while considering only statistical longitudinal and lateral offsets.

Thus, the performance of several layouts of a typical avionics SI-POF link, with different number of connectors will be analyzed using the propagation matrix framework combined with the upgraded connector model to simplify and speed up the simulations. Statistical distributions of power loss and bandwidth in the different scenarios will be extracted from the resulting output power distributions and frequency responses to assess the impact of the number and position of the connectors.

2. STATISTICAL CONNECTOR MISALIGNMENT MODEL

The simulated system was a 42-meter fiber link made up of several segments of Mitsubishi GH4002 SI-POF with different lengths that were joined by a number of ST connectors. In particular, three configurations were tested using one, two and five connectors, respectively. The first configuration consisted of two 21-meter segments joined by a single ST connector. In the second configuration three 14-meter segments were joined by two ST connectors. The last configuration consisted of six 7-meter segments with 5 connectors. In addition, the simulation of a fiber link without connectors was also calculated to serve as a reference. Fig. 1 shows the schematic representation of all these configurations.

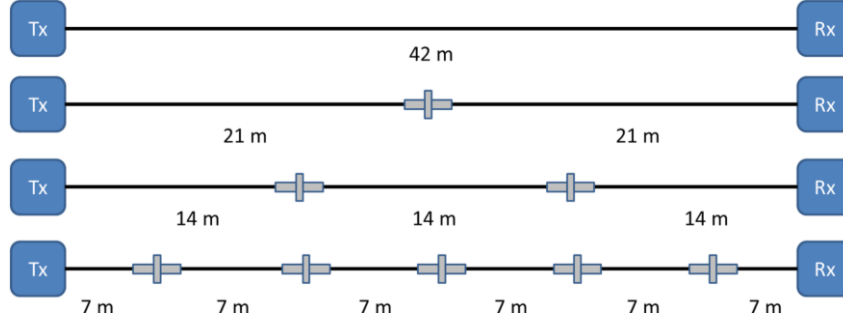


Figure 1. Schematic of the four 42-meter link configurations with different number of connectors.

The model used to describe the fiber and the misaligned connectors with misalignments is not detailed here, as it has been thoroughly described previously. The POF segments were modeled as matrices using the propagation matrix model [11] to solve the diffusion equation. The connectors were also described by matrices whose angular attenuation depends on the lateral and longitudinal misalignment that is obtained with a method based on the Hankel Transform [6]. The use of matrices simplifies and speeds up calculations, which is very beneficial for the proposed Monte Carlo simulation. The angular power distribution launched into the fiber was modelled using measurements obtained for the transmitter of a commercial transceiver from Firecomms based on a VCSEL emitting at 645 nm [12]. Finally, the receiver was modelled as a wide area detector whose driver electronics circuit poses no extra limitation to the fiber frequency response. This assumption is reasonable as the simulated fiber length is quite large and thus it is the major contributor to characteristics of the frequency response.

Randomness was introduced in the simulations by allowing each instance of the connector model to be configured with simultaneous and independent lateral (x_0 and y_0) and longitudinal (z_0) misalignments that were drawn from Gaussian distributions whose standard deviation was $\sigma = 31.25 \mu\text{m}$ according to the tolerances defined in IEC-60793-2-40 specifications, A4a.2 fiber class. We assumed that connectors have an air gap and thus, the mean value of z_0 was $150 \mu\text{m}$. A simulation run with $N = 5 \cdot 10^3$ simulation samples was obtained for each link configuration shown in Fig. 1. Each simulation sample was the result of propagating the optical power from the transmitter to the receiver through a number of fiber segments joined by ST connectors. All the characteristic parameters of the link: input power distribution, fiber properties, detector position, etc. were deterministic. Only the connectors' shifts in the three spatial dimensions (x_i, y_i, z_i for connector i) were Gaussian random variables that further led to Gaussian-distributed longitudinal misalignments and Rayleigh-distributed radial misalignments [10]. Power loss and bandwidth measurements were obtained from the output power distribution and the system frequency response of each simulation sample. Standard deviations of these parameters are plotted as a function of the number of samples in Fig. 2, confirming that the number of samples was enough to reach a stable distribution in the three tested scenarios.

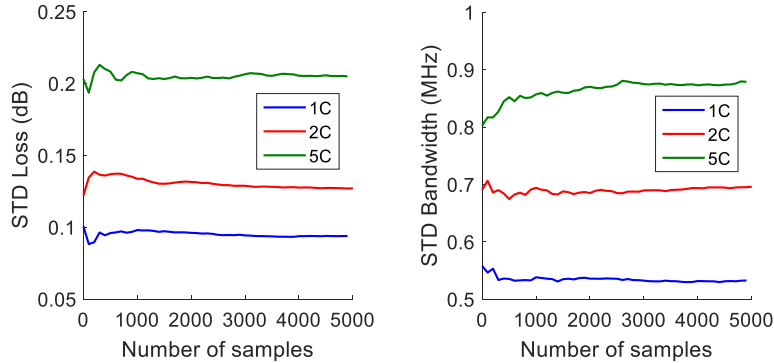


Figure 2. Evolution of standard deviation of power loss (left) and bandwidth (right) versus number of samples.

3. IMPACT ON OVERALL LINK PERFORMANCE

Results from all the simulation samples were processed in order to statistically characterize the effect of the connector misalignments over the main transmission parameters. Average and standard deviations of output power distribution and frequency response were obtained and the probability density functions of power loss and bandwidth were estimated.

3.1 Impact over angular power distribution and power loss

In Fig. 3, the average and standard deviation of the output angular power distribution is shown on the right for the three configurations and the reference link (without connectors). From these functions, the encircled area flux (EAF) was calculated and its mean is shown on the left graph together with the input EAF (dotted line).

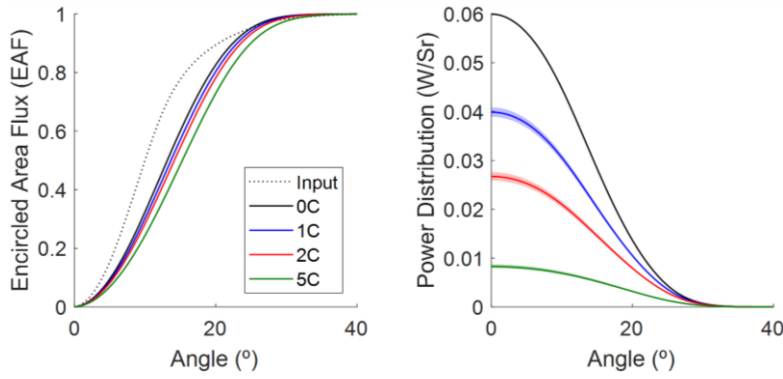


Figure 3. EAF (left) and power distributions (right) for the three configurations and the reference link (0C).

As the plots show, the resulting standard deviations are very low showing that connector misalignments introduce only very small variations in the spatial power distribution. The differences in the shapes of the EAFs obtained for the different configurations are also small, but significant and reveal that the pattern is wider as the number of connectors increases. On the other hand, the right graph shows a drastic decrease of the maximum power as the number of connectors increases justified by their high insertion loss since we are dealing with air-gap connectors with mean fiber-to-fiber offsets of $150\ \mu\text{m}$. The total output power was obtained from each sample of the output power distribution to calculate power loss in dB for each configuration. The resulting data were used to obtain empirical probability density functions (pdf) and cumulative distribution functions (cdf) for the three configurations, as shown in Fig. 4. We found that the resulting power loss statistical distributions fit reasonably with extreme value distributions with increasing mean and standard deviation values as the number of connectors increases.

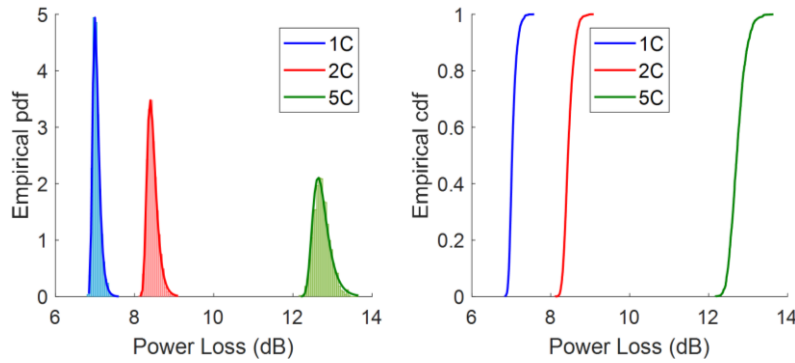


Figure 4. Output optical power statistical distribution for the three configurations: empirical probability density function and fitting to extreme value distribution (left) and empirical cumulative distribution function (right).

3.2 Impact on frequency response and bandwidth

The effects of connector variability due to misalignments on the frequency response and system bandwidth are illustrated in Fig. 5. Mean and standard deviation of normalized frequency responses for the three configurations, as well as for the reference link, are plotted on the left graph, while the center and right plot show the empirical probability density and cumulative distribution functions for the 3-dB bandwidth, respectively.

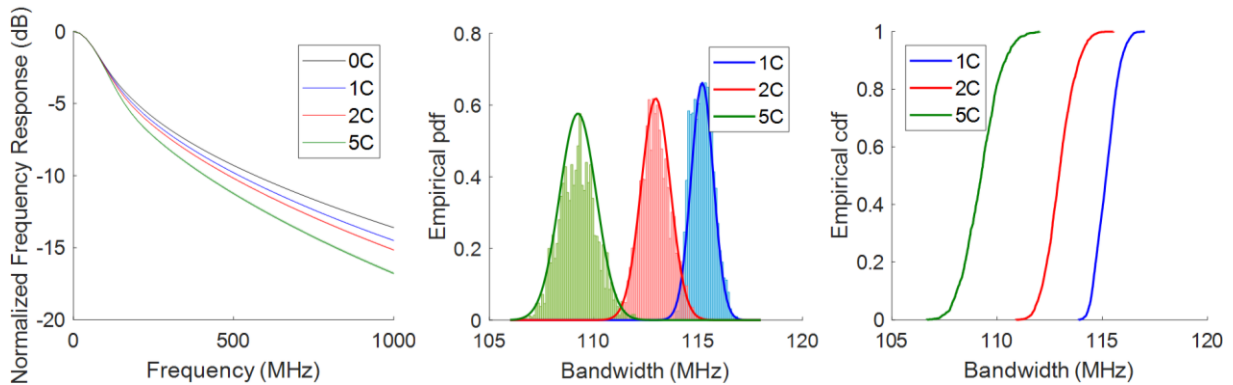


Figure 5. Average and standard deviation of the normalized frequency responses (left), and empirical probability density and cumulative distribution functions of the bandwidth (center and right, respectively).

The frequency responses show significant degradation that increases with the number of connectors in the system as the left graph shows. The variability introduced by connector misalignment is, however, small. Regarding the statistical behavior of the bandwidth, the empirical probability density functions (pdf) are more symmetrical than those obtained for power loss and can be fitted to Gaussian distributions as shown in the center plot. Both, pdf and cumulative distribution functions reveal how the bandwidth decreases when increasing the number of connectors while its standard deviation increases. The values of the mean, the standard deviation and the 97th percentile are shown in Table 1 for all configuration tested.

Table 1. Mean, standard deviation and 97th percentile of power loss and bandwidth for the simulation results.

Link configuration	Power loss (dB)			3-dB Bandwidth (MHz)		
	Mean	Std. Dev.	97 th percentile	Mean	Std. Dev.	97 th percentile
1 connector (1C)	7.0395	0.0932	7.2554	115.1968	0.5325	116.2558
2 connectors (2C)	8.4549	0.1270	8.7223	112.9683	0.6970	114.3315
5 connectors (5C)	12.7332	0.2040	13.1474	109.2420	0.8787	110.9444

4. DISCUSSION

The values of the average and standard deviation of power loss and bandwidth as a function of the number of connectors are plotted in Fig. 6 in red and green, respectively. As the number of connector increases, average power loss is higher as should be expected while the average bandwidth is lower. The power loss and bandwidth for a 42-meter POF link without connectors is also shown in the corresponding graphs. The standard deviation is relatively small for both parameters but increases as more connectors are introduced in the link.

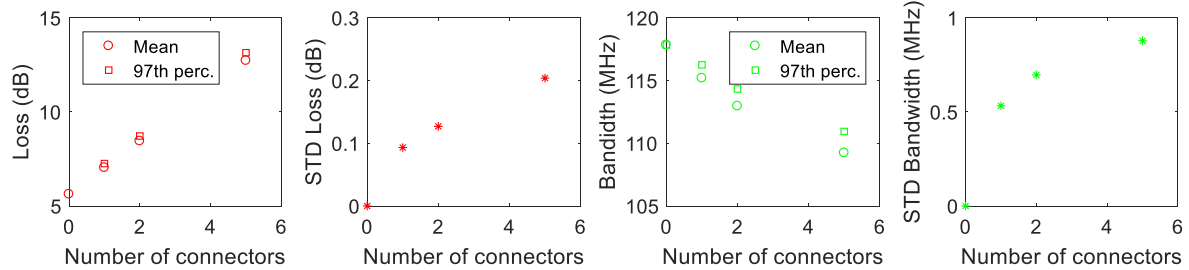


Figure 6. Mean, standard deviation, and 97th percentile of power loss and bandwidth vs number of connectors.

The decrease of link bandwidth with the number of connectors is explained by their broadening effect over the power distribution demonstrated by the EAFs shown in Fig. 3. Power at higher propagation angles is transmitted at lower speed through the fiber degrading its frequency response. Thus, it seems that, as the EAF broadening increases with the number of connectors, the bandwidth decreases. This effect has been reported and is particularly intense when the connector is close to the transmitter where it behaves as a mode scrambler broadening the power distribution [4,6]. However, it has also been reported that connectors near the receiving end can even improve link performance [6], particularly, those with an air-gap [13]. Therefore, we set out to quantify the effect of the position of the connector in the link for the case of only one connector. Thus, four new configurations have been tested inserting the connector closer to both the receiver and the transmitter: 3.5, 7, 35 and 38.5 meters from the transmitter (the latter two are 7 and 3.5 meters from the detector, respectively). These results are compared to the one that we presented before where the single connector is placed in the middle of the 42-meter link and also, to the case with no connectors. The results are plotted in Fig. 7, showing that the EAF, the spatial power distribution and the mean and standard deviation of the estimated probability density functions of power loss are practically identical and independent of the connector position in the link. The standard deviation of the EAF and the power distribution for all conditions are also very small.

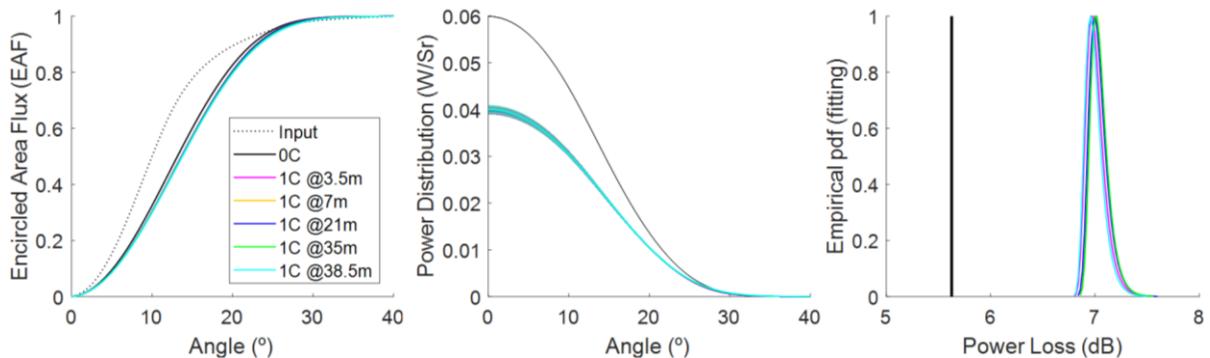


Figure 7. Average and standard deviation of EAF (left) and spatial power distribution (center) and empirical pdf of power loss (right) for one-connector configurations. The black line is for a 42-m fiber without connectors.

On the other hand, Fig. 8 shows the frequency responses and the estimated probability density function and cumulative distribution function of the bandwidth for all one-connector configurations. The frequency responses on the left graph show differences that are significant in spite of the variability introduced by connector misalignments. These differences are more evident in the probability distribution of the bandwidth values for the different conditions. The center plot shows that as the connector moves closer to the input, the bandwidth reduction is larger. However, when the connector is closest to the detector, the bandwidth is significantly higher than for the condition without connectors, which is represented by the black line. This effect is consistent with a filtering of higher order modes that is achieved through the air-gap in the connector.

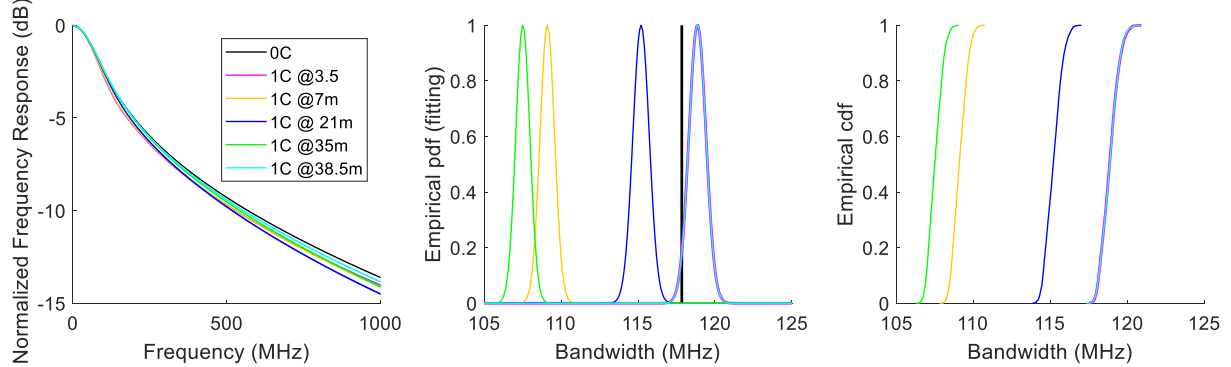


Figure 8. Average and standard deviation of the normalized frequency responses (left), and estimated pdf and cdf (center and right, respectively) of the bandwidth for one connector at different positions.

Table 2 shows the average, standard deviation and 97th percentile of power loss and bandwidth obtained for the five different configurations with one connector. The frequency responses, however, present significant differences that reflect on the bandwidth values obtained from them. The standard deviations of the power loss and bandwidth distributions do not change with the connector position.

Table 2. Mean, standard deviation and 97th percentile of power loss and bandwidth for the different positions.

Distance from Tx	Power loss (dB)			3-dB Bandwidth (MHz)		
	Mean	Std. Dev.	97 th percentile	Mean	Std. Dev.	97 th percentile
21 m (REF)	6.9976	0.0727	7.2554	115.1970	0.5325	116.2558
3.5 m	7.0123	0.0691	7.2728	107.4890	0.4515	108.4136
7.0 m	7.0068	0.0700	7.2573	109.0900	0.4648	110.0149
35.0 m	6.9695	0.0731	7.2200	118.8470	0.5424	119.9489
38.5 m	6.9571	0.0704	7.1930	118.8490	0.5401	119.9292

Fig. 9 shows the values of the average and standard deviation of power loss (red plots) and bandwidth (green plots) as a function of the connector distance to the transmitter. This figure summarizes our conclusions about the influence of the connector position on these parameters. As the distance between the connector to the transmitter decreases, bandwidth values also decrease. Bandwidth standard deviation increases proportionally to its average. However, power loss does not change significantly with connector position.

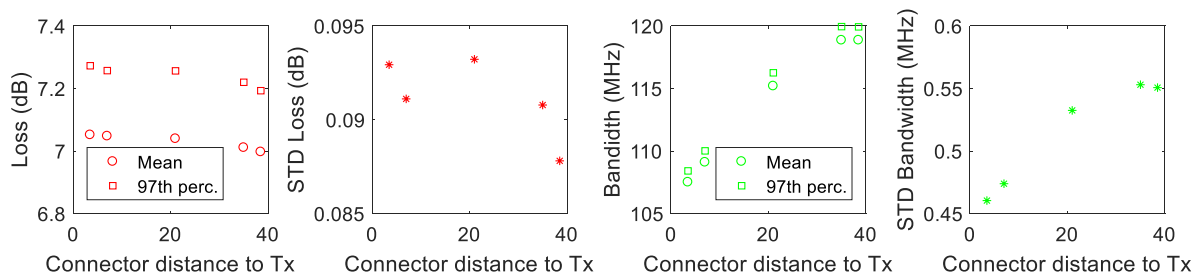


Figure 9. Mean and standard deviation of power loss and bandwidth as a function of the connector position.

As a summary, a plot of the bandwidth versus power loss values for all configurations tested is shown in Fig. 10. This graph shows that the effect of connector position over bandwidth is quite strong. The presence of one connector near the detector, increases the bandwidth values compared to the value for the fiber only, while if the connector is near the transmitter, the degradation is even larger than that produced by 5 connectors. The increase of the number of connectors also degrades performance but, in the case of the 5 connectors, the degradation introduced by the previous connector is partially filtered by the last connector, which is at 7 meters from the detector. Power loss is independent of connector position and increases linearly with the number of connectors, as is the case for its standard deviation.

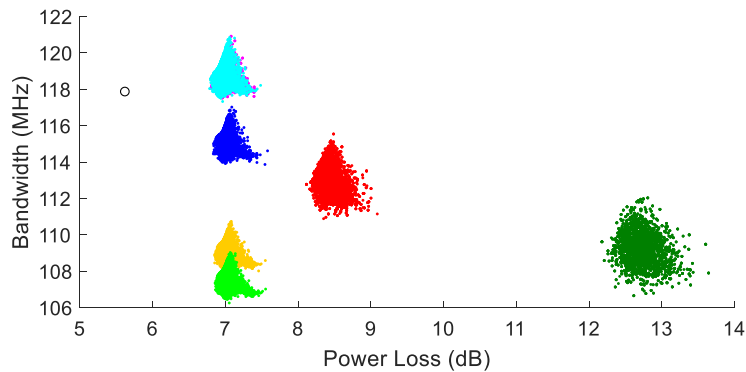


Figure 10. Results on bandwidth and power loss obtained from all the simulated configurations.

5. CONCLUSIONS

We used Monte Carlo simulations to assess the variability of POF transmission properties in a typical avionics system due to statistical connector misalignments. A matrix framework was used to model the fiber and connectors. The use of the SI-POF matrix model combined with the upgraded connector matrix simplifies the testing of different designs and allows us to obtain not only power loss, but also power distributions, frequency responses and bandwidths. The analysis of the simulation results provides not only the mean and standard deviation of power distributions and frequency responses, but also estimates of the probability and cumulative density functions. As the number of connectors increases, power loss increases and bandwidth decreases. The standard deviations of both properties also increase with the number of connectors. On the other hand, changes in the connector position do not alter spatial properties but has a significant impact on frequency response and bandwidth.

ACKNOWLEDGEMENTS

This work has been funded by Fondo Europeo de Desarrollo Regional (FEDER), Spanish Ministerio de Ciencia, Innovación y Universidades, Agencia Estatal de Investigación under grant RTI2018-094669-B-C33 (MICINN/FEDER), by Gobierno de Aragon (DGA), under grant T20_17R, and by the National Science Foundation (NSF) under the GOALI grant 1809242.

REFERENCES

- [1] O. Ziemann, *et al.*: Application of Polymer Optical and Glass Fibers, in *POF Handbook: Optical Short Range Transmission Systems*, Ed., Springer, 2nd edition, 2008.
- [2] M. A. Losada, *et al.*: Influence of Termination on Connector Loss for Plastic Optical Fibres, in *Proc. ICTON 2014*, Graz, Austria, 2014.
- [3] A. Esteban, *et al.*: Effects of connectors in SI-POFs transmission properties studied in a matrix propagation framework, in *Proc. ICPOF 2011*, Bilbao, Spain, 2011.
- [4] E. Grivas, *et al.*: Influence of Connectors on the Performance of a VCSEL-Based Standard Step-Index POF Link, *IEEE Photon. Technol. Lett.*, vol. 21, no. 24, pp. 1888-1890, 2009.
- [5] S. Kobayashi, *et al.*: Evaluation of Modal Power Distribution of Automotive Optical Gigabit Ethernet Connections, *J. Lightw. Technol.*, vol. 35, no. 17, pp. 3664-3670, 2017.
- [6] J. Mateo, *et al.*: POF misalignment model based on the calculation of the radiation pattern using the Hankel transform, *Opt. Express*, vol. 23, no. 6, pp. 8061-8072, 2015.
- [7] D. H. Richards, *et al.*: Modeling Methodology for Engineering SI-POF and Connectors in an Avionics System, *J. Lightw. Technol.*, vol. 31, no. 3, pp. 468-475, 2013.
- [8] P. V. Mena, *et al.*: Using system simulation to evaluate design choices for automotive Ethernet over plastic optical fiber, *Proc. of SPIE*, vol. 10560, 2018.
- [9] S. Werzinger, *et al.*: An Analytic Connector Loss Model for Step-Index Polymer Optical Fiber Links, *J. Lightw. Technol.*, vol. 31, no. 16, pp. 2769-2776, 2013.
- [10] S. Werzinger, C. A. Bunge: Statistical analysis of intrinsic and extrinsic coupling losses for step-index polymer optical fibers, *Opt. Express*, vol. 23, no. 17, pp. 22318-22329, 2015.
- [11] J. Mateo, *et al.*: Frequency response in step index plastic optical fibers obtained from the generalized power flow equation, *Opt. Express*, vol. 17, pp. 2850-2860, 2009.
- [12] A. López, *et al.*: On the Variability of Launching and Detection in POF Transmission Systems, in *Proc. ICTON 2018*, Bucharest, Romania, 2018.
- [13] N. A. Albakay, L. Nguyen: Achieving 1 Gbps Over Step-Index Plastic Optical Fiber Using Spatial Mode Air-Gap Filter, *IEEE Photon. Technol. Lett.*, vol. 29, no. 8, pp. 655-658, 2017.